15th Canadian Masonry Symposium
Ottawa, Canada
June 2-5, 2025

Comparative Analysis of Alternative Supplementary Cementitious Materials for Potential Application in Concrete Masonry Units

Shanjida Khan[i], Ali Teymouri[ii], Saeid Ghasemalizadeh[iii], and Rahil Khoshnazar[iv]

ABSTRACT

Portland cement plays a major role in concrete masonry units (CMUs) as a binding agent; however, cement production contributes to high amounts of greenhouse gas emissions. A widely adopted strategy for reducing such emissions is the use of supplementary cementitious materials (SCMs) as partial replacements for cement. However, the increasing scarcity of conventional SCMs, such as fly ash and slag, has necessitated the need to explore alternative SCMs (ASCMs). Therefore, this research aims to compare the effects of two ASCMs, namely reclaimed fly ash (RFA) and recycled glass powder (RGP), on the properties of cementitious mixtures. Cement paste and mortar samples with 20 wt% cement replacement by these ASCMs were prepared, and tested for rheology, heat of reactions, flow table, and compressive strength development. The results were compared to a reference sample containing 100 wt% cement and a sample with 20 wt% cement replacement with Class F fly ash (FA). The results showed that the RFA did not considerably affect the flowability of cementitious mixtures as determined by the apparent viscosity of the pastes and flow table measurements of the mortars. Incorporating RGP slightly increased these parameters compared to the reference samples made with only cement. The total heat evolution of the pastes incorporating these ASCMs over the 7-day testing period was lower than that of the reference, with the heat of the paste with RGP being marginally higher than that of RFA and FA. The mortars with RFA and RGP had reduced compressive strength at early ages, however, this diminished by 91 days, when compared to the reference mortar and that with FA. These findings provide a basis for implementation of these ASCMs into CMUs to reduce their cement content while maintaining or improving their mechanical properties, contributing to the development of low-carbon CMUs.

KEYWORDS

alternative supplementary cementitious materials, cement mortar, compressive strength, heat of reaction, rheology

[i] M.Sc. Student, University of Calgary, Calgary, Canada, shanjida.khan1@ucalgary.ca
[ii] PhD Candidate, University of Calgary, Calgary, Canada, ali.teymouri@ucalgary.ca
[iii] Postdoctoral Researcher, University of Calgary, Calgary, Canada, saeid.ghasemalizadeh@ucalgary.ca
[iv] Associate Professor, University of Calgary, Calgary, Canada, rahil.khoshnazar@ucalgary.ca

INTRODUCTION

Concrete masonry units (CMUs) are widely used in the construction industry due to their durability, load-bearing capacity, and versatility. However, the production of Portland cement, a key component of CMUs, is associated with significant energy consumption and greenhouse gas (GHG) emissions, contributing to approximately 8 to 9% of global anthropogenic CO_2 emissions and 2 to 3% of energy demand annually [1]. Utilization of supplementary cementitious materials (SCMs) to partially replace Portland cement in CMUs has been a viable option to lower the associated GHG emissions [2]. Fly ash (FA), a widely used SCM in concrete production, is a by-product from the combustion of coal in electrical power plants [3]. For CMUs, one study revealed that at 20 vol% FA, masonry block samples fulfilled the criteria for load-bearing and non-load-bearing applications [4]. However, due to its scarcity as coal-fired power plants are phasing out [5], exploring alternative SCMs (ASCMs) is imperative. Furthermore, there is a gap in understanding the comparative performance between different ASCMs.

One promising ASCM is reclaimed fly ash (RFA), sourced from FA stored in landfills and repurposed for cementitious applications. The effect of incorporating RFA on the fresh and hardened properties of cementitious mixtures, including flow properties which is influenced by particle size and angularity of the ASCM, varies depending on the source of the material [6]. In a study performed by Al-Shmaisani et al. [6], two types of RFA were incorporated into cement paste and both pastes were found to have higher viscosity than that with FA, all at 20 wt% replacement level, however, the yield stress fluctuated between the two pastes with RFA in comparison to the one with FA [6]. Another ASCM gaining attention is recycled glass powder (RGP), produced by sorting, crushing, and pulverizing waste glass [7]. The incorporation of RGP has been found to result in a slight reduction in slump with increasing RGP replacement levels. This could be attributed to the irregular shape and smaller particle size of RGP compared to regular Portland cement [8]. The heat flow of cement paste incorporating RGP varies according to the literature, however, one study found the peak heat to be comparable to the reference when normalized to the weight of cement at 10, 25, 35, and 60 wt% replacement levels [9]. Studies also show varying compressive strength results on mortar incorporation of RGP, with some studies displaying similar results to the control, at early and late ages, while others show decreases of up to 25% [8], [10]. As RFA and RGP have shown varying results with the incorporation into cementitious mixtures, it is important to investigate its properties to establish its efficacy for potential use in CMUs while reducing waste in landfills.

This study focuses on the incorporation of RFA and RGP into cement paste and mortar, addressing the gap in understanding their comparative performance on the rheology, hydration kinetics, flow, and compressive strength with a brief discussion on the environmental considerations. By comparing locally sourced RFA and RGP with conventional FA, this research investigates their viability as an ASCM. This study evaluates key properties of ASCMs in cementitious mixtures to provide a framework for scaling up the research for application in CMUs.

MATERIALS AND METHODS

Materials Selection

The cement used in this research was general use Portland limestone cement (PLC), type GUL complying with Canadian standard (CSA A3001:23) [11]. The recycled glass powder (RGP) was procured from a company in the USA, in compliance with ASTM C1866-20 [12]. Reclaimed fly ash (RFA) was obtained locally from Alberta, Canada, made from repurposed landfilled fly ash. Class F fly ash (FA) was also provided by a Canadian company.

The main oxide composition and loss on ignition (LOI) of the cementitious materials tested in this study are presented in Table 1. The particle size distribution was collected through the laser diffraction technique and presented in Figure 1. Deionized water was used for all mixing procedures, and standard graded silica sand conforming to ASTM C778-21 [13], from Humboldt USA, was used in preparing mortar samples.

Table 1: Main oxide compositions and loss of ignition of the GUL cement, Class F fly ash, reclaimed fly ash, and recycled glass powder (wt.%).

Material	SiO_2	Al_2O_3	CaO	Fe_2O_3	MgO	SO_3	K_2O	Na_2O	LOI
GUL cement	18.30	3.93	60.81	3.34	4.16	3.43	0.36	0.06	5.02
Class F fly ash	54.96	23.23	10.99	3.59	1.14	0.23	0.74	2.58	1.15
Reclaimed fly ash	59.59	22.52	8.21	3.58	0.96	0.19	0.70	1.81	1.78
Recycled glass powder	64.54	7.35	16.26	0.27	3.35	0.06	0.08	5.91	0.96

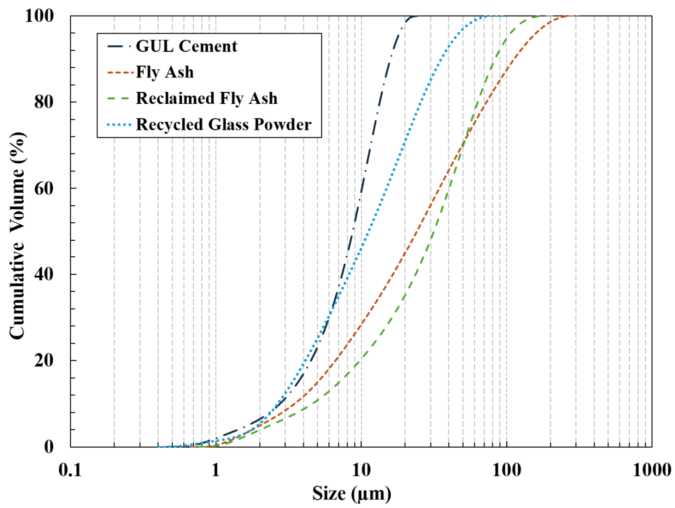

Figure 1: Particle size distribution of GUL cement, Class F fly ash, reclaimed fly ash, and recycled glass powder.

Sample preparation

Four cement paste and four mortar samples were prepared in this study. The proportion of cementitious materials used in these mixtures is presented in Table 2. The “P” and “M” in the mixture ID denote cement paste and mortar samples, respectively. The cementitious mixtures in this study included one reference mixture with 100 wt% PLC (REF), and three mixtures with 20 wt% of PLC replaced with each of the SCMs. The cement pastes were used for rheology and isothermal calorimetry tests. Mortar samples were used for flow table measurement at the fresh state, and compressive strength testing at 3, 7, 28, and 91 days.

Table 2: Proportion of cementitious materials in cement paste and mortar mixtures (wt.%).

Mixture ID	GUL cement	Class F fly ash	Reclaimed fly ash	Recycled glass powder
P-REF/M-REF	100	-	-	-
P-20FA/M-20FA	80	20	-	-
P-20RFA/M-20RFA	80	-	20	-
P-20RGP/M-20RGP	80	-	-	20

Cement pastes were prepared in accordance with ASTM C305-20 [14] with a water-to-cementitious materials (w/cm) ratio of 0.42. Mortar samples were prepared according to ASTM C109-21 [15] (w/cm ratio of 0.485 and sand-to-cementitious materials ratio of 2.75) for compressive strength testing. The cement paste and mortar mixtures containing SCMs were prepared by dry mixing PLC and 20 wt% PLC replacement with SCM for 30 seconds prior to adding it to water. The mortar samples were mixed in accordance with ASTM 305-20 [14] and tested for flow table. Mortar samples were cast into 50 mm × 50 mm × 50 mm cubic samples and sealed cured for the first 24 hours. Upon demoulding, they were placed in a fog room with a relative humidity of 95 ± 5% and temperature of 23 ± 2 °C to cure until the testing age approached.

Testing Procedures

Rheology

The rheology of the cement pastes was measured using a modular compact rheometer (MCR302, Anton Paar, Austria) with a serrated bob and cup system. Fresh paste was added to the device cup after 15 minutes of the water and dry cementitious materials coming into contact to ensure it had entered its dormant stage [16]. A flow test was conducted to measure the changes in shear stress against different shear rates. The shear rates applied were: 150, 100, 80, 60, 40, 20, 10, 1 and 0.1 rotations per second. The test protocol consisted of pre-shearing the cement paste for 75 seconds at 150 s^{-1}, followed by a gradual reduction in the applied shear rates maintained for 15 to 30 seconds at each shear rate to achieve equilibrium. The collected shear stresses, at the shear rates induced, were then plotted and fitted to the best fit line obtained by the Bingham model, modified Bingham model, and Herschel-Bulkley model [17]. In this study, the Herschel-Bulkley model, shown below in **Error! Reference source not found.**), was the best fit for all the cement paste samples.

(1) $\tau = \tau_0 + K^* \gamma^n$

Where, τ is the shear stress in Pa, τ_0 is the yield stress in Pa, K is the consistency index, n is the flow index, and γ is the shear rate from the rotational speed of the device [18]. The apparent viscosity of the pastes was also calculated by dividing the shear stress by the shear rate and plotted.

Isothermal Calorimetry

Isothermal calorimetry was conducted using an isothermal microcalorimeter (TAM Air, TA instruments, USA) in accordance with ASTM C1702-23 [19]. Cement pastes were prepared based on the thermal mass of quartz sand, which were added to the reference channels to establish a baseline 20 hours prior to adding in the tested samples. Approximately 40 g of paste samples was prepared, and about 10 g of fresh cement paste was added to glass ampoules and placed into the testing cells of the calorimeter five minutes after the water and dry cementitious mixture came into contact. The heat evolution of the samples was recorded over 7 days after adding the samples to the cells, using the TAM Assistant software.

Flow Table

Flow table test was conducted on the fresh mortar samples based on ASTM C1437-20 [20]. This was conducted to understand the flowability of fresh mortar samples with the incorporation of the different SCMs/ASCMs.

Compressive Strength

Compressive strength test was conducted at 3, 7, 28, and 91 days as per ASTM C109-21 [15]. The test was performed using a compressive strength device (Compressive Strength Tester, RIEHLE, USA). At each age, three mortar samples were tested and the average and standard deviation of the strength measurements were reported.

Results and Discussion

Rheology

Figure 2 presents the flow curves of the cement pastes, obtained by measuring their shear stress at different shear rates. The data points in Figure 2 represents the experimental data collected for each sample and the lines display the Herschel-Bulkley model along with their equations. The n values, or the flow index, which are denoted by the exponent on the equations in Figure 2, revealed that the flow indices are all less than one, demonstrating shear-thinning behaviour of these pastes.

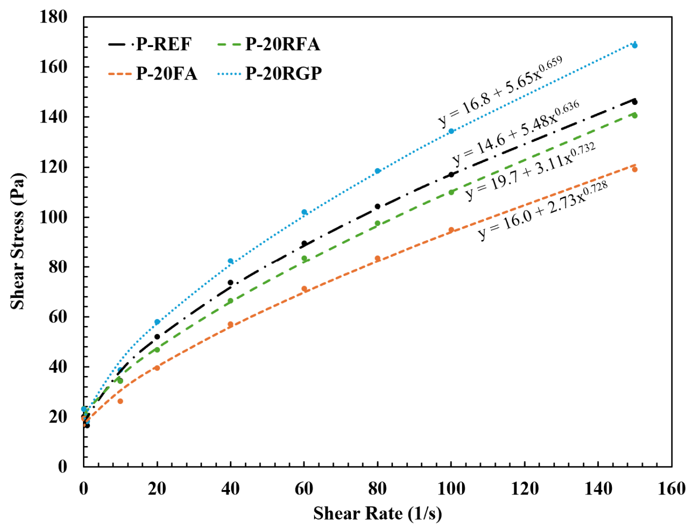

Figure 2: Shear stress versus shear rate for different cement pastes, with the corresponding Herschel-Bulkley equations displayed on each curve.

The apparent viscosity of all the cement paste samples are presented in Figure 3. Replacing 20 wt% PLC with FA reduced the viscosity of the cement paste by almost 20%. For the paste with the same amount of RFA, however, the decrease in the viscosity was marginal and this paste (P-20RFA) had a comparable viscosity to that of P-REF, especially at higher shear rates. This is consistent with the results reported by Al-Shmaisani et al. [6], where the viscosity of their cement paste sample (w/cm of 0.45) with 20 wt% FA was the lowest (0.12 Pa.s), followed by the cement paste with RFA (0.15 Pa.s) while the reference paste with only cement had the highest viscosity (0.19 Pa.s) [6].

The paste with 20 wt% (P-20RGP) sample had an increase of ~15% in apparent viscosity compared to P-REF. This is consistent with a similar study done by Lu et al. [21], where cement paste, with a w/cm ratio of 0.4, incorporating 20 wt% cement replacement with RGP led to a significant increase in plastic viscosity compared to a reference mixture with 100 wt% cement [21]. Comparison of the apparent viscosity measurements for the pastes with SCMs/ASCMs suggests that at all shear rates the paste with RGP had the highest viscosity followed by the paste with RFA and then the one with FA. At the highest shear rate (150 s^{-1}), the difference between P-20RGP and P-20FA was almost 35%. The increased viscosity of RGP compared to FA and RFA could be due to the finer particle size of RGP compared to FA and RFA, shown in Figure 1, along with other particle characteristics [22].

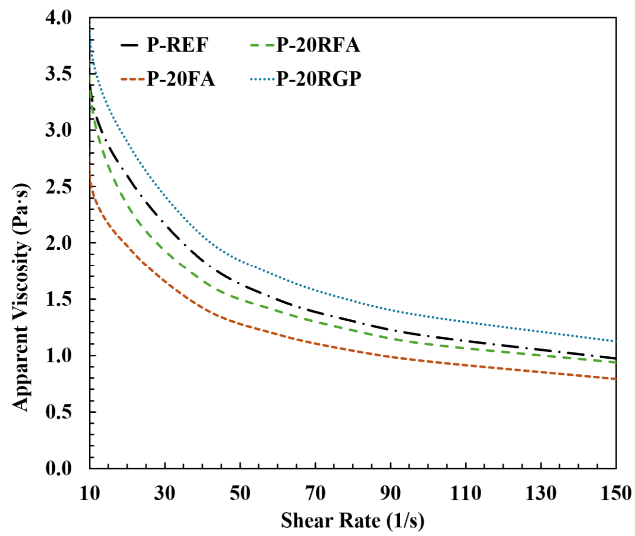

Figure 3: Apparent viscosity at different shear rates of cement pastes using the Herschel-Bulkley model.

Isothermal Calorimetry

Figure 4 displays the heat flow, in mW/g, and cumulative heat, in J/g, of paste samples over a testing period of 7 days. In Figure 4a, the parameters are normalized to the weight of cement and in Figure 4b they are normalized to the weight of binder. The P-REF sample presented two peaks in the heat flow curve. The initial peak, which is more prominent, indicated the reaction of tri-calcium silicate (C_3S) in the cement, which occurred at 8.4 hours with a peak heat flow of 3.2 mW/g cement. The second, less prominent peak occurring in between 12 to 18 hours, during the descending part of the curve, was related to secondary ettringite formation from the reaction of tri-calcium aluminate (C_3A) and gypsum in the cement [23].

The incorporation of FA at 20 wt% of the cement in the paste, P-20FA, slightly decreased the peak heat flow (3.0 mW/g cement), which occurred at a later time (9.4 hours) compared to that observed for P-REF. The P-20RFA sample experienced a relatively comparable and delayed peak heat flow compared to P-REF, with a peak heat flow of 3.1 mW/g cement at 8.8 hours, however, P-20RFA had a marginally higher heat flow to that of P-20FA. Diaz-Loya et al. [24], found that the heat flow of cement paste incorporating RFA and FA, at 20 wt% cement replacement led to a reduced peak heat compared to a reference with 100 wt% cement, at w/cm ratio of 0.4. However, their results indicated that the cement paste with FA had a higher peak heat flow than RFA [24], which differs from the results of this study.

The P-20RGP sample exhibited the same peak heat flow of 3.2 mW/g cement, compared to P-REF, at 8.6 hours, revealing that the P-20RGP sample had similar hydration kinetics compared to P-REF. Compared to P-20FA and P-20RFA, the P-20RGP had a marginal increase in the peak heat flow. The heat flow normalized to binder (Figure 4b) shows a more pronounced decrease in the observed peak for P-20FA, P-20RFA, and P-20RGP due to the dilution effect of utilizing SCMs/ASCMs.

The P-REF sample had the highest cumulative heat when normalized to binder throughout the testing period. The cumulative heat of P-20FA had a decrease of 17% at 7 days compared to P-REF mainly due to the dilution effect of cement replacement. The P-20RFA sample experienced a similar cumulative heat to that of P-20FA. The cumulative heat was 14% lower for P-20RGP than that of P-REF at 7 days. Furthermore, the cumulative heat of P-20RGP was marginally higher than that of P-20FA and P-20RFA. When normalized to the weight of cement (Figure 4a), the cumulative heat of the cement pastes with the cement replacements appeared to be greater than that of P-REF, as this only accounts for the cement content, which was added at a lower amount in these pastes compared to P-REF.

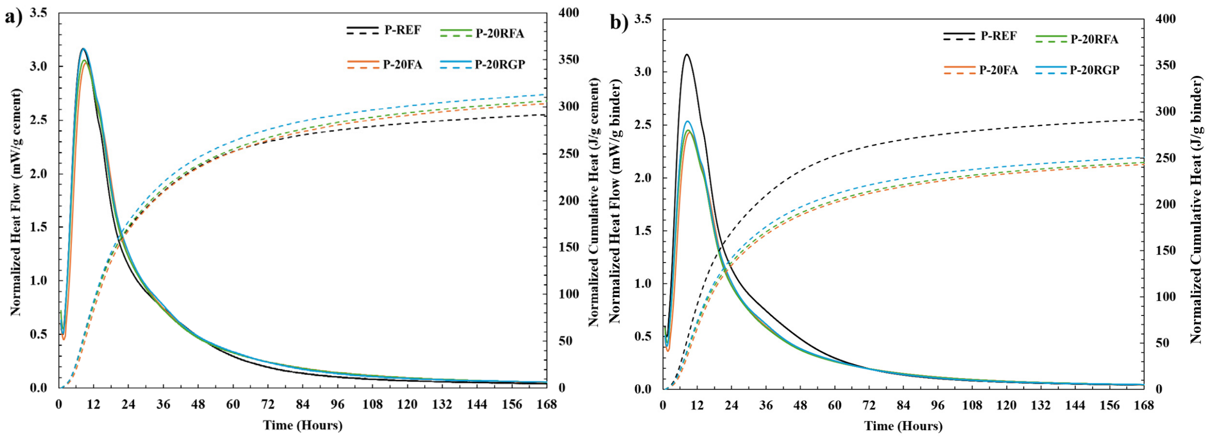

Figure 4: Heat flow and cumulative heat over 7 days for cement pastes, a) normalized to the weight of cement, b) normalized to the weight of binder.

Flow table

Flow table results of the mortar samples are presented in Figure 5. The M-REF sample had a flow table result of 96 %. The mortar sample with 20 wt% PLC replacement with FA, M-20FA, sample had a flow of 102 %, which was higher than the remaining mortar samples. This is common for FA due to its particle size distribution [25], and smooth and spherical particle shape, which reduces the friction between the particles and making it easier to flow within cementitious mixtures [26]. M-20RFA flow was comparable to M-REF, with a result of 98 %. This is consistent with the apparent viscosity results where the sample containing RFA had values closer to the reference. The M-20RGP sample reduced the flow slightly compared to M-REF and had a flow table result of 93 %. This is also consistent with the viscosity results, where the sample with RGP exhibited a slight increase in apparent viscosity compared to the reference. Overall, the effect of utilizing the ASCMs on the flow of the mortars appeared to be marginal, making them practical for industrial applications.

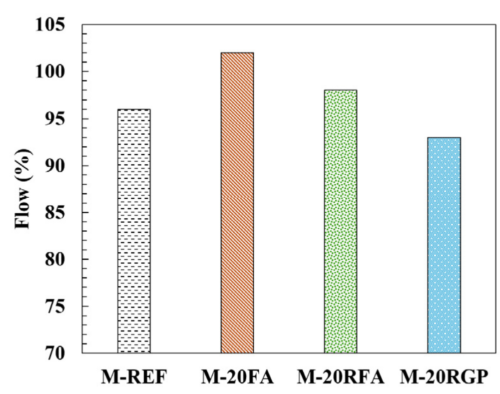

Figure 5: Flow table results of mortar samples.

Compressive Strength

The compressive strength results for the mortar samples at the ages of 3, 7, 28, and 91 days are presented in Figure 6. As shown in the figure, the mortar with 100 wt% PLC, M-REF, had a compressive strength of

23.0 MPa, and 27.9 MPa, at the ages of 3 and 7 days, respectively. At 28 days, M-REF achieved a compressive strength of 35.7 MPa, with no further significant strength gain at 91 days (36.3 MPa). Replacing the PLC by 20 wt% with FA, in M-20FA, decreased the compressive strength of the mortar by 10 to 15% at the ages of 3 to 28 days. However, by 91 days, the compressive strength of M-20FA reached that of M-REF, due to the pozzolanic reactions of FA. In the case of M-20RFA, the compressive strength was lower than that of the M-REF by ~ 20% to 24% at the ages of 3 to 28 days, with marginal decrease observed at 91 days. Compared to M-20FA, the M-20RFA sample showed a slight decrease in compressive strength at the ages of 3, 7, and 28 days. The difference in compressive strength of M-20RFA and M-20FA was marginal at 91 days.

The M-20RGP sample had a 21% decrease in compressive strength at 3 days, however, at 7 and 28 days, M-20RGP only had a slight decrease in strength, compared to M-REF. At 91 days, the compressive strength of M-20RGP slightly surpassed M-REF, with a strength of 39.2 MPa compared to 36.3 MPa obtained for the M-REF. The M-20RGP sample had comparable compressive strength results at 7 and 28 days to M-20FA, and, at 91 days, the compressive strength of M-20RGP exceeded that of M-20FA, even though the increase was only 3.0 MPa. Comparing the compressive strength of the samples with ASCMs, M-20RGP and M-20RFA had the same compressive strength at 3 days. At 7, 28, and 91 days, the M-20RGP sample exceeded the compressive strength of M-20RFA by 22%, 18% and 15%, respectively. Overall, both ASCMs demonstrated significant potential to provide comparable or enhanced compressive strengths of cementitious mixtures at later ages.

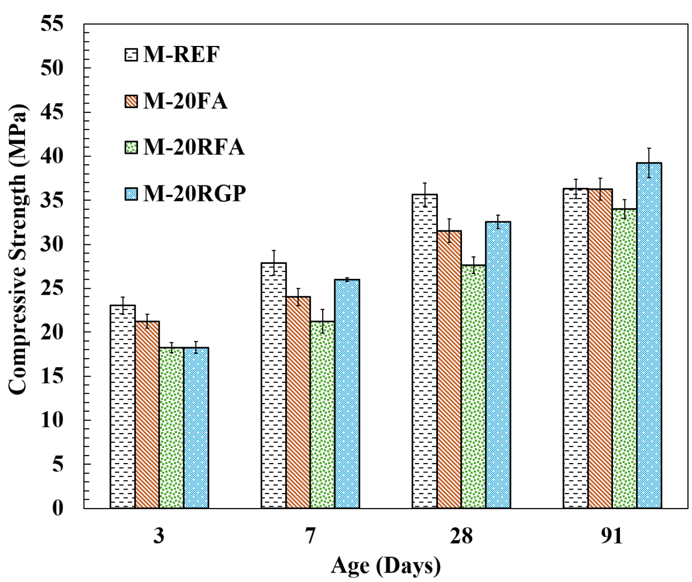

Figure 6: Compressive strength of mortar samples at 3, 7, 28, and 91 days.

Environmental Impact Considerations

The utilization of RGP and RFA as ASCMs showed potential, with consistent flow properties between cement paste and mortar, reduced total heat of reactions, and comparable compressive strength at later ages, at 20 wt% PLC replacement. These highlight the practicality of incorporating these ASCMs into CMUs, potentially offering environmental benefits. As ASCMs reduce the Portland cement content, they pose a solution to reduce GHG emissions. For example, in a cradle-to-grave life cycle assessment (LCA) performed in 2018, glass powder used at 20 wt% Portland cement replacement and was found to have a 20% reduction in GHG emissions compared to concrete with no Portland cement replacement [27]. Along with decreasing the reliance on the Portland cement clinker, the use of RFA and RGP also reduce landfill waste, which has been found to have cost benefits [28] in addition to the environmental ones.

When utilizing industrial by-products or wastes, key considerations include the processing requirements and associated transportation emissions. The processing of RGP, for example, involves grinding which could be energy-intensive, to achieve particle sizes suitable for use as an ASCM [29]. This additional energy consumption can contribute to GHG emissions, the magnitude of which depends on regional electricity generation practices, as electricity is used in most cases for grinding. For instance, in Alberta, 49% of electricity generation is from coal-fired power plants, followed by 38% from natural gas, 7% from hydropower and the remaining 6% from wind and biomass energy sources, which could result in higher GHG emissions compared to regions with cleaner energy sources to produce electricity [30]. The regional phase-out of coal-fired power plants also affects the availability of RFA, which necessitates the transportation of RFA over long distances, potentially negating the environmental benefits due to fuel consumption and emissions [28]. As well, RGP for this study was sourced from the USA, so it is important to consider the emissions due to transportation. This is because GHG emissions related to the transportation of materials in concrete production can contribute to 20% of the total [31]. However, these emissions also depend on the source of the fuel required for transportation.

A comprehensive LCA that considers the consistency in performance when ASCMs are incorporated into CMUs, processing requirements, regional electricity generation emissions, and transportation impacts is necessary to fully evaluate the environmental advantages and disadvantages of utilizing RGP and RFA for CMUs.

CONCLUSION

In this study, the incorporation of RFA and RGP into cementitious mixtures as 20 wt% replacements for PLC was investigated through a comparative analysis in terms of their rheology, heat of reaction, flow, and compressive strength, with a brief discussion about the environmental considerations. These properties were also compared to a reference sample with no PLC replacement and a sample with the same content of PLC replacement with FA to understand their potential as ASCMs for practical applications. The key findings from this study are:

- The incorporation of RFA, at 20 wt% PLC replacement, did not considerably change the apparent viscosity of the paste while the incorporation of the same content of FA reduced the viscosity of the paste by almost 20% and the incorporation of RGP increased it by ~15%, compared to the reference. The flow table results of the mortar also showed comparable measurement for the RFA and the reference mortar with only PLC, slightly higher measurement for the mortar with FA, and marginally lower measurement for the one with RGP.
- The cement paste samples had marginal differences in heat flow curves, when normalized to the weight of cement, showing similar hydration kinetics at early ages. The cumulative heat over the 7-day testing period, normalized to the weight of binder, of all the samples with PLC replacements had a decrease when compared to the reference.
- The mortar samples incorporating RFA and RGP at 20 wt% PLC replacement exhibited a decrease in compressive strengths at early ages with comparable results at the age of 91 days, to the reference mortar. Comparing both mortar samples with ASCMs, both had the same strength at 3 days, while, at later ages, the mortar with RGP had a higher compressive strength than that of the mortar with RFA.
- The use of industrial wastes or by-products in CMUs has potential to reduce GHG emissions, conserve natural resources and reduce waste in landfills. However, factors such as, consistency in

performance, and emissions due to regional energy, transportation, and processing, need to be considered.

The findings highlight the potential of utilizing RFA and RGP in place of FA, especially due to the limited availability of FA and provide a basis for implementation of ASCMs in CMUs. The benefits extend to other concrete industry sectors by revealing that the utilization of these ASCMs could increase or decrease flowability depending on the application, reduce heat of reaction which can prevent thermal cracking, and provide comparable ultimate compressive strengths.

ACKNOWLEDGEMENTS

The authors gratefully acknowledge the financial support provided by the Natural Sciences and Engineering Research Council of Canada (NSERC), facilitating the research presented in this study. The authors also extend their gratitude to Lafarge Canada for providing the cement.

REFERENCES

[1] Monteiro, P., Miller, S. & Horvath, A. (2017) Towards sustainable concrete. *Nature Materials*. 16, 698–699.

[2] Najaf, E., & Abbasi, H. (2022). Using Recycled Concrete Powder, Waste Glass Powder, and Plastic Powder to Improve the Mechanical Properties of Compacted Concrete: Cement Elimination Approach. *Advances in Civil Engineering*, 2022.

[3] Jayaranjan, M.L.D., van Hullebusch, E.D. & Annachhatre, A.P. (2014). Reuse options for coal fired power plant bottom ash and fly ash. *Rev Environ Sci Biotechnol* 13, 467–486.

[4] Turgut, P. (2010). Masonry composite material made of limestone powder and fly ash. *Powder Technology*, 204(1), 42–47.

[5] Ozcelikci, E., Kul, A., Gunal, M. F., Ozel, B. F., Yildirim, G., Ashour, A., & Sahmaran, M. (2023). A comprehensive study on the compressive strength, durability-related parameters and microstructure of geopolymer mortars based on mixed construction and demolition waste. *Journal of Cleaner Production*, 396, 136522.

[6] Al-Shmaisani, S., Kalina, R. D., Ferron, R. D., & Juenger, M. C. G. (2019). Evaluation of beneficiated and reclaimed fly ashes in concrete. *ACI Materials Journal*, 116(4), 79–87.

[7] Chandra Paul, S., Šavija, B., & Babafemi, A. J. (2018). A comprehensive review on mechanical and durability properties of cement-based materials containing waste recycled glass. *Journal of Cleaner Production*, 198, 891–906.

[8] Nahi, S., Leklou, N., Khelidj, A., Oudjit, M. N., & Zenati, A. (2020). Properties of cement pastes and mortars containing recycled green glass powder. *Construction and Building Materials*, 262, 120875.

[9] Jochem, L. F., Casagrande, C. A., Onghero, L., Venâncio, C., & Gleize, P. J. P. (2021). Effect of partial replacement of the cement by glass waste on cementitious pastes. *Construction and Building Materials*, 273, 121704.

[10] Mejdi, M., Wilson, W., Saillio, M., Chaussadent, T., Divet, L., & Tagnit-Hamou, A. (2022). Hydration and microstructure of glass powder cement pastes – A multi-technique investigation. *Cement and Concrete Research*, 151, 106610.

[11] CSA A3001 (2023). Cementitious materials compendium. CSA Standard.

[12] ASTM C1866 (2020). Standard specification for ground-glass pozzolan for use in concrete. ASTM International Standard.

[13] ASTM C778 (2021). Standard specification for standard sand. ASTM International Standard.

[14] ASTM C305 (2020). Standard practice for mechanical mixing of hydraulic cement pastes and mortars of plastic consistency. ASTM International Standard.

[15] ASTM C109 (2020). Standard test method for compressive strength of hydraulic cement mortars (using 2-in. or [50-mm] cube specimens). ASTM International Standard.

[16] John, E., & Lothenbach, B. (2023). Cement hydration mechanisms through time – a review. *Journal of Materials Science*, 58 (24), 9805–9833.
[17] Zhang, C., Wang, M., Liu, R., Li, X., Liu, Y., Jiang, P., Yan, J., Zhu, Z., & Chen, M. (2023). Rheological properties of cement-based slurry and evaluation of rheological model: Influence of particle size and shape. Construction and Building Materials, 406, 133498.
[18] Nehdi, M., & Rahman, M. A. (2004). Estimating rheological properties of cement pastes using various rheological models for different test geometry, gap and surface friction. *Cement and Concrete Research*, 34(11), 1993–2007.
[19] ASTM C1702 (2023). Standard test method for measurement of heat of hydration of hydraulic cementitious materials using isothermal conduction calorimetry. ASTM International Standard.
[20] ASTM C1437 (2020). Standard test method for flow of hydraulic cement mortar. ASTM International Standard.
[21] Lu, J. X., Shen, P., Zhang, Y., Zheng, H., Sun, Y., & Poon, C. S. (2021). Early-age and microstructural properties of glass powder blended cement paste: Improvement by seawater. *Cement and Concrete Composites*, 122, 104165.
[22] Youness, D., Yahia, A., & Tagnit-Hamou, A. (2022). Development of viscosity models of concentrated suspensions: Contribution of particle-size and shape indices. *Construction and Building Materials*, 346, 128335.
[23] Scrivener, K. L., Juilland, P., & Monteiro, P. J. M. (2015). Advances in understanding hydration of Portland cement. *Cement and Concrete Research*, 78, 38–56.
[24] Diaz-Loya, I., Juenger, M., Seraj, S., & Minkara, R. (2019). Extending supplementary cementitious material resources: Reclaimed and remediated fly ash and natural pozzolans. *Cement and Concrete Composites*, 101, 44–51.
[25] Mehdipour, I., & Khayat, K. H. (2017). Effect of particle-size distribution and specific surface area of different binder systems on packing density and flow characteristics of cement paste. *Cement and Concrete Composites*, 78, 120–131.
[26] Michael, T. (2013). Supplementary Cementing Materials in Concrete. CRC Press.
[27] Deschamps, J., Simon, B., Tagnit-Hamou, A., & Amor, B. (2018). Is open-loop recycling the lowest preference in a circular economy? Answering through LCA of glass powder in concrete. *Journal of Cleaner Production*, 185, 14–22.
[28] Huang, T. Y., Chiueh, P. T., & Lo, S. L. (2017). Life-cycle environmental and cost impacts of reusing fly ash. Resources, *Conservation and Recycling*, 123, 255–260.
[29] Magni Darwich Higuchi, A., Gorett dos Santos Marques, M., Farias Ribas, L., & Pereira de Vasconcelos, R. (2021). Use of glass powder residue as an eco-efficient supplementary cementitious material. *Construction and Building Materials*, 304, 124640.
[30] Farhat, A. A. M., Ugursal, V. I. (2010) Greenhouse gas emission intensity factors for marginal electricity generation in Canada. *International Journal of Energy Research*, 34 (15), 1309-1327.
[31] Pacheco, A. A. L., Oliveira, L. S., John, V. M., Angulo, S. C. (2022). Transportation impact on CO2 emissions of concrete: a case study in Rio Branco/Brazil., *Revista ibracon de estruturas e materials*., 15 (6).